Journal of Materials Chemistry A

Facile preparation of yttrium and aluminum co-doped ZnO via sol-gel route for photocatalytic hydrogen production

Journal:	*Journal of Materials Chemistry A*
Manuscript ID:	TA-COM-05-2014-002207.R1
Article Type:	Communication
Date Submitted by the Author:	15-May-2014
Complete List of Authors:	Huo, Jingpei; South China University of Technology, School of Chemistry and Chemical Engineering, State Key Laboratory of Luminescent Materials and Devices, Institute of Functional Molecules Fang, Li; South China Normal University, School of Chemistry and Environment Lei, Ya; South China Normal University, School of Chemistry and Environment Zeng, Gong; South China University of Technology, School of Chemistry and Chemical Engineering, State Key Laboratory of Luminescent Materials and Devices, Institute of Functional Molecules Zeng, He; South China University of Technology, School of Chemistry and Chemical Engineering, State Key Laboratory of Luminescent Materials and Devices, Institute of Functional Molecules

Cite this: DOI: 10.1039/c0xx00000x

www.rsc.org/xxxxxx

ARTICLE TYPE

Facile preparation of yttrium and aluminum co-doped ZnO via sol-gel route for photocatalytic hydrogen production

Jingpei Huo[a], Liting Fang[b], Yaling Lei[b], Gongchang Zeng[a] and Heping Zeng*[a]

Received (in XXX, XXX) Xth XXXXXXXXX 20XX, Accepted Xth XXXXXXXXX 20XX

DOI: 10.1039/b000000x

Yttrium and aluminum co-doped ZnO was successfully synthesized by the sol-gel method, showing high photocatalytic activity for hydrogen production (5.71 mmol*h^{-1}*g^{-1}) in the water/lactic acid system under visible-light irradiation for the first time, exhibiting excellent stability and recyclability.

As a kind of unique metal oxide,[1, 2] because of its excellent optical and electrical properties, zinc oxide (ZnO) is potential for a variety of practical applications including semiconductors, field-effect transistors, luminescence, solar cells, gas sensors, photodetectors, UV-blocking and other aspects.[3-7] Besides, ZnO has become a promising photocatalyst, owing to its lower cost, flexible preparation method, non-toxicity, high photosensitivity, chemical and thermal stability.[8-12] Thus, more and more scientists are attracted to the intensive research on the photocatalytic H_2 production with ZnO recently.[13, 14] While ZnO has a wide band gap of 3.2 eV and responds only to the UV part of the solar spectrum.[15, 16] As a result, it is very desirable to enhance the photoactivity of ZnO and extend its light absorption capability into the visible region.[17, 18]

It is well known that semiconductor coupling, dye sensitization, and metal, non-metal or co-doping have been applied to develop visible light sensitive ZnO.[5, 19, 20] Among them, many reports on doping of ZnO with metals such as copper (Cu)[21], indium (In)[22] and lanthanum (La)[23] are available, resulting in the modification of their band gap, but there are relatively few using ZnO doped with aluminium (Al)[24], yttrium (Y)[25] or co-doped ZnO. Noticably, Al and Y have been found to be very efficient for visible light induced photocatalysis because they can make the energy band gap decrease, promoting the surface segregation and the surface enrichment, improving the photocatalytic performance.[25, 26] Various methods such as hydrothermal process, sol-gel method and co-precipitation method have been reported for the synthesis of undoped or doped ZnO nanoparticles (NPs).[27] In these approaches, sol-gel is the most effective and facile method to prepare the NPs.[23, 28]

However, to the best of our knowledge, Al and Y co-doped ZnO has never been synthesized by sol-gel and used for the field of photocatalytic hydrogen production. Based on our previous research,[29-31] we report a modified sol-gel method to fabricate ZnO NPs embedded by Al and Y, driven by vacuum annealing (see Experimental details in the ESI†). The resulting ZnO NPs are characterized by X-ray diffraction (XRD), scanning electron microscopy (SEM), Brunauer-Emmett-Teller (BET), UV-vis and photoluminescence (PL) spectroscopies. Futhermore, their photocatalytic activities are investigated under visible light irradiation.

The purity and crystallinity of as-synthesized samples was investigated by XRD, and the results are displayed in **Fig. 1a** and **1b**. **Fig. 1a** shows the XRD patterns of aluminum-doped zinc oxide (AZO) NPs with different Y doping ratios. All diffraction peaks were in good agreement with the JCPDS No. 36-1451.[32] As can be seen from these patterns, the diffraction peaks of yttrium and aluminum co-doped ZnO (Y-AZO) NPs were broader and slightly shifted towards a lower Bragg angle than that of pure AZO. When the doping amount of Y was changed from 1% to 5%, no characteristic peak from other crystalline was detected. For Y loaded more than 7%, the Y-AZO NPs have an additional peak located at around 29.41°, corresponding to the (111) plane of cubic Y_2O_3 (JPCDS no. 43-0661).[33] The peak indicates that the presence of Y_2O_3 for the Y-AZO NPs.

On the other hand, **Fig. 1b** shows the XRD patterns of yttrium-doped zinc oxide (Y-ZnO) NPs with different Al doping ratio. It can be clearly seen that the diffraction peaks of aluminum and yttrium co-doped ZnO (Al-Y-ZnO) NPs become sharper with an increasing amount of Al, leading to the increase of the particles size and the improvement of the crystalline.[24] According to **Fig. 1b**, it was typically observed that a preferred orientation along the (101) crystal plane, showing a high crystallinity.[24] The peak heights of Y_2O_3 decreased a little, even disappeared, as the Al concentration increased. The reason may be that the replacement of Y by Al in the ZnO lattice. The XRD patterns further demonstrate the synthesis of Al-Y-ZnO NPs.

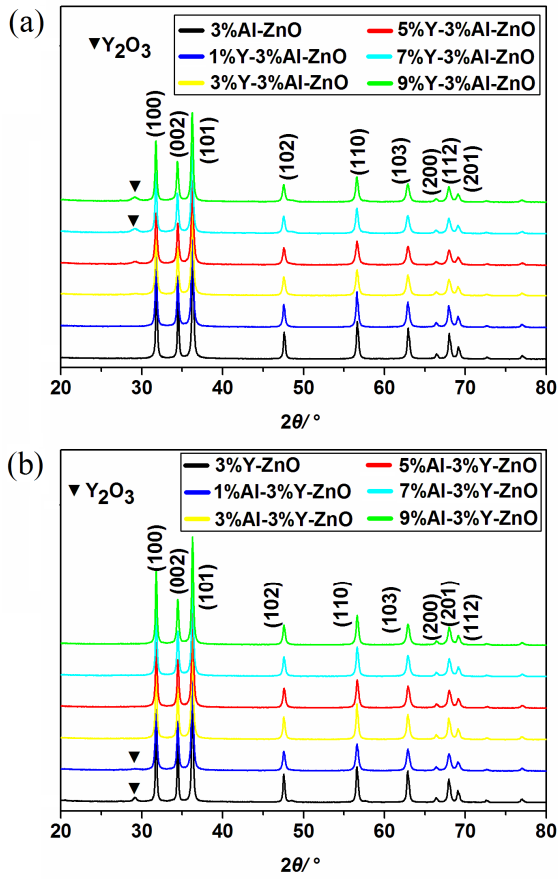

Fig. 1 XRD patterns of the as-synthesized ZnO NPs: (a) the different doping amount of Y, (b) the different doping amount of Al.

The morphologies and particle sizes of the representative samples were examined by using SEM analysis (**Fig. 2a-2d**). SEM images in **Fig. 2a and 2b** show that the samples have fine particles. It can be seen that the diameters of the particles lie in the range of 20-30 nm for all two samples. While the Y doped amount was increased, the structure of ZnO crystallites gradually form granule-like rough conformations with the particles sizes decreased as shown in **Fig. 2c** and **2d**. Futher observation in **Fig. 2c** and **2d** shows that for Y loading higher than 7%, the sample was irregularly agglomerated approximately particles, even for the segregation of excess Y. These findings are consistent with the above results from **Fig. 1** indeed, and Y-doping seems to have an effect on the crystal growth of AZO. Thus, it may be briefly summarized that the doping and the doping amount of Y influence the crystallite size. Also, the high doping incites the morphological change and the additional formation of the Y-AZO phase.

Meanwhile, the elemental nature of catalysts was investigated with energy dispersive spectra (EDS). EDS of AZO and Y-AZO are shown in **Fig. 2e** and **2f**. EDS of AZO reveals that the sample contains mainly three elements (Zn, Al and O). EDS of Y-AZO shows Y as one extra element.

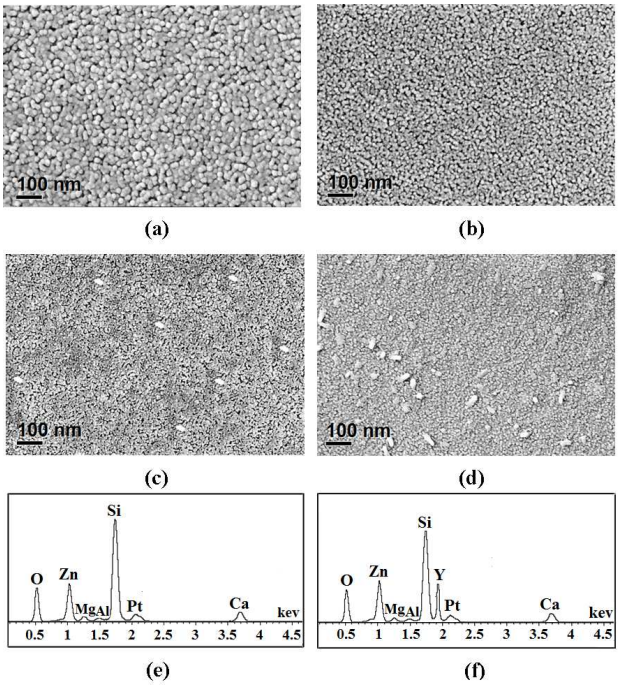

Fig. 2 SEM images of Y-AZO NPs: (a) 3%Y-3%Al-ZnO, (b) 5%Y-3%Al-ZnO, (c) 7%Y-3%Al-ZnO, (d) 9%Y-3%Al-ZnO; EDS spectrums of: (e) AZO NPs, (f) Y-AZO NPs.

The photocatalytic hydrogen evolution activities of all the prepared samples were investigated under visible light irradiation with an aqueous lactic acid (LA) solution, as presented in **Fig. 3** and **Table 1**. No hydrogen gas was produced when the experiment was performed by taking pure LA solution in the absence of either photocatalyst or irradiation.[34] **Fig. 3a** and **Table 1** show the hydrogen evolution rate of pure ZnO NPs, AZO NPs, Y-ZnO NPs, Y-AZO NPs and commercial P25, respectively. Obviously, the hydrogen evolution rate of pure ZnO NPs is the lowest among them. This can be attributed to two reasons, one is the limited light absorption ability, another one is the rapid recombination rate of electron-hole pairs.[35] AZO NPs was observed to be higher activity compared to undoped ZnO. It is worth mentioning that the hydrogen production activity is enhanced slightly when Al are deposited on ZnO. In the system of AZO NPs, the introduction of Al on the surface can accelerate the division and restrain the recombination of photogenerated electron-hole pairs, resulting in improved photocatalytic activity.[36, 37] A similar trend was also found for the hydrogen production activity of Y-ZnO NPs, and its hydrogen evolution rate is 1.61 $mmol*h^{-1}*g^{-1}$ (**Fig. 3a**). The reason is that the Y acts as a cocatalyst which can facilitate the catalytic hydrogen production on the ZnO edge sites through photoelectron excitation.[25] Significantly, Y-AZO NPs achieves a maximum value at about 3.58 $mmol*h^{-1}*g^{-1}$. This value is higher than the sum of the hydrogen evolution rate of pure ZnO NPs (0.18 $mmol*h^{-1}*g^{-1}$), AZO NPs (1.36 $mmol*h^{-1}*g^{-1}$), Y-ZnO NPs (1.61 $mmol*h^{-1}*g^{-1}$) and commercial P25 (0.072 $mmol*h^{-1}*g^{-1}$), as illustrated in **Fig. 3a** and **Table 1**. These results demonstrate that the incorporation of Y with the AZO NPs favors the improvement of its photocatalytic activity. It is noted to be that Y and Al have positive synergetic effects on

the hydrogen production activity of ZnO NPs.

From **Table 1**, it is observed that Y-AZO NPs obtain the highest apparent quantum efficiency (QE) of 2.31% at 420 nm among all investigated photocatalysts, including 0.10% for ZnO, 1.24% for AZO, 1.33% for Y-ZnO, and 0.04% for commeral P25 (for calculation details of QE see ESI†).

In addition, there is a difference in BET specific surface area (S_{BET}), as given in **Table 1**. Among all the prepared photocatalysts, Y-AZO exhibits the largest surface area of 118.5 m^2/g. Y-AZO has more active sites on the surface for adsorption of reactant molecules, and that might be the reason why it shows the highest photocatalytic activity.[22]

The effect of different Y dopant concentrations on the photocatalytic H_2 production using Y-AZO was studied under identical experimental conditions for three hours (**Fig. 3b**). In **Fig. 3b** it is clear that the optimum photocatalytic performance was obtained for 5%Y-AZO, reaching 5.71 $mmol*h^{-1}*g^{-1}$.The hydrogen production activity of Y-AZO NPs increases initially with increasing amounts of Y and reach amaximum H_2 production rate at the optimal dopant concentration. Whereas a further loading in the amount of Y, the hydrogen evolution rate progressively decays. Probably, the reason for this phenomena is that the light filtrated by the excess Y, the high agglomeration of Y may block the active sites on the surface of the Y-AZO NPs, and the deterioration of the catalytic properties of Y at their enlargement.[38, 39] Hence, the 5%Y-AZO NPs was the best performing sample and was selected for the following recycling experiments.

To investigate the stability and recyclability of the developed photocatalysts, the time course of photocatalytic hydrogen production over 5%Y-AZO was carried out in six cycles (24 h), as shown in **Fig. 3c**. Remarkably, it exhibited a linear relationship with irradiation time during the entire experimental period and no obvious loss of activity after six cycles, indicating that hydrogen production is persistent for continuous operation.[40] Consequently, it is an exceptionally efficient and stable photocatalyst in such experimental conditions, which can be applied for industrial clean energy production.

To characterize the optical properties of ZnO, AZO, Y-ZnO and Y-AZO, UV-Vis absorption and PL measurements were performed at room temperature (**Fig. 4**). As shown in **Fig. 4a**, a characteristic absorption sharp edge for pure ZnO is at around 410 nm due to its intrinsic wide band-gap, suggesting that it has limited light absorption ability for itself.[35] On the contrary, AZO shows a strong absorption in the whole wavelength range (300-500 nm) due to the dopant of Al. Al can modify the surface of ZnO and enhance the surface electric charge of ZnO, promoting the enhancement of light capture.[36, 37] In particular, Y-AZO NPs show a stronger absorption than ZnO and AZO in the whole light region (**Fig. 4a**). This also proves that both Al and Y NPs are effective co-catalysts for ZnO from the previous photocatalytic hydrogen evolution experiment, further contributing to the enhanced photocatalytic activity.

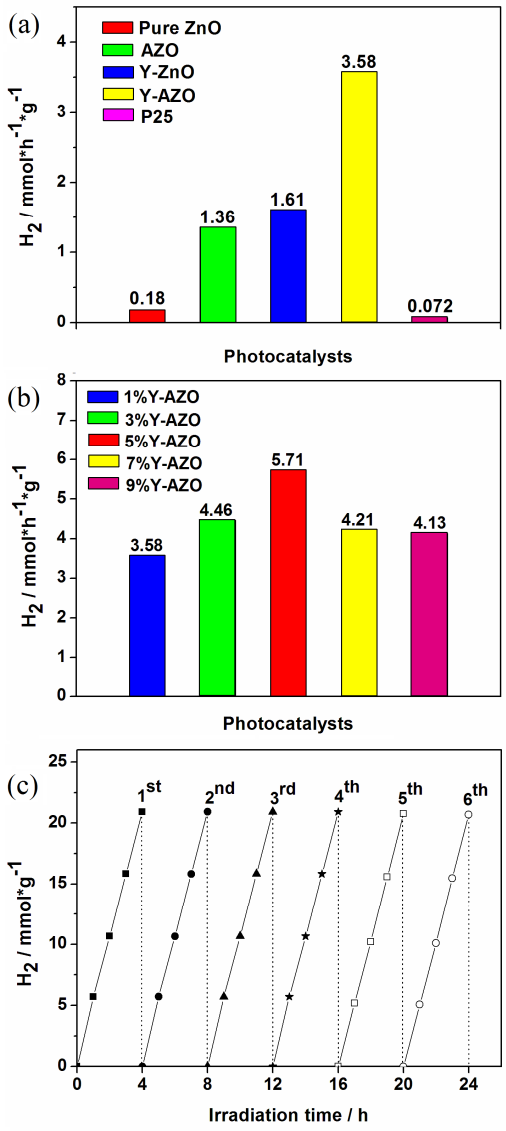

Fig. 3 Photocatalytic activity of the as-prepared samples (0.05 g) in an aqueous solution (60 mL) containing LA (10 mL) under visible-light irradiation: (a) hydrogen evolution rate of pure ZnO, AZO, Y-ZnO, Y-AZO and P25, respectively (irradiation time = 3 h); (b) effect of different Y dopant concentrations on the photocatalytic H_2 production using Y-AZO (irradiation time = 3 h); (c) long-term hydrogen production activity of 5%Y-AZO NPs (irradiation time = 24 h).

Table 1 The hydrogen production rate, QE and S_{BET} of as-prepared photo-catalysts

Sample	H_2[a]/mmol*h^{-1}*g^{-1}	QE[b]/%	S_{BET} (m_2*g^{-1})
Pure ZnO	0.18	0.10	61.9
AZO	1.36	1.24	77.1
Y-ZnO	1.61	1.33	82.7
Y-AZO	3.58	2.31	118.5
P25	0.072	0.04	45.2

[a]Reaction was conducted under a 300 W Xe arc lamp with a ultraviolet cut-off filter; 0.05 g of each catalyst was dispersed in the above conditions.

[b]QE was calculated based on the amounts of H_2 evolved under monochromatic light irradiation (λ = 420 nm) in 1 h.

In order to verify the above discussion, the PL spectra of selected samples were carried out with excitation at 260 nm

(**Fig. 4b**). PL analysis can be regarded as another key approach to understand the charge separation property of the photocatalysts.[26, 35] The higher PL intensity would represent a high rate of electron-hole recombination.[22, 35] Namely, the more intense the PL emission peak is, the more it hinders the photocatalytic activity.[22] It can be clealy seen that ZnO exhibits a more intense PL peak than others from **Fig. 4b**, demonstrating that a maximum recombination of electron-holes in the pure ZnO sample, leading to the decrease of photocatalytic activity. Also, from **Fig. 4b**, it can be shown that combining ZnO with Al or Y NPs can bring about a clear diminution of the PL emission, because either Al or Y can trap photo-generated electrons through the interface to facilitate the charge separation.[36, 37, 41]

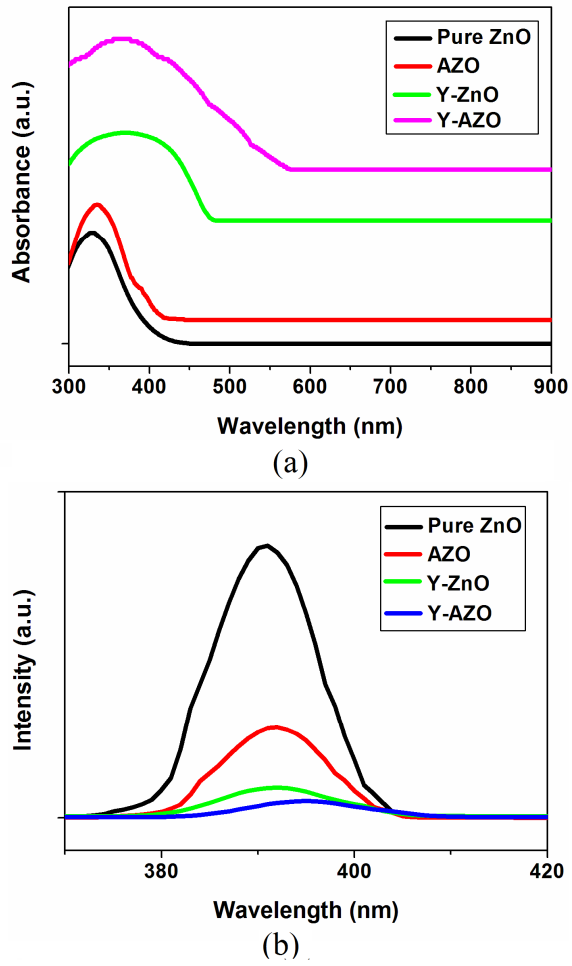

Fig. 4 (a) UV-vis and (b) PL spectra of pure ZnO, AZO, Y-ZnO and Y-AZO, respectively.

Moreover, Al and Y can favour the electrons reaching the surface of ZnO easily to initiate the photocatalytic reaction, and enhance the photocatalytic activity.[22] It should be also noted that the decrease of PL intensity may be affected by both surface and bulk defects,[42, 43] which is matched with the above results from the BET analysis. It is worth noting that the cooperation of Al and Y can minimize the recombination of charge carriers in the Y-AZO system. All these factors suggest that both the strongest light absorption ability and the most effective charge separation ability for Y-AZO NPs can lead to the highest efficiency of photocatalytic hydrogen production indeed as expected.

In conclusion, Y-AZO NPs were successfully synthesized and well characterized by XRD, SEM, EDS, BET, UV-vis and PL. Among all the prepared samples, the best photocatalytic performance is observed for 5%Y-AZO NPs. It shows an extremely fast hydrogen evolution rate of 5.71 mmol*h^{-1}*g^{-1}, and possesses high reusability. This work clearly demonstrates that both Y and Al NPs in the Y-AZO system for light absoption, electron transfer and catalysis for a highly cooperative solar production of hydrogen gas from LA solution. Besides, Y-AZO NPs can be compelling photocatalysts for photocatalytic water splitting, and provide new insight for modifications of ZnO.

Acknowledgements

We are grateful to the National Natural Science Foundation of China (No. 21371060) for financial support. We thank Benjamin J. Deibert for proofreading this article.

Notes and references

[a]*State Key Laboratory of Luminescent Materials and Devices, Institute of Functional Molecules, School of Chemistry and Chemical Engineering, South China University of Technology, Guangzhou, 510641, P. R. China. Fax: 86-20-87112631; Tel: 86-20-87112631; E-mail: hpzeng@scut.edu.cn.*
[b]*School of Chemistry and Environment, South China Normal University, Guangzhou, 510006, P. R. China.*

† Electronic Supplementary Information (ESI) available: Experimental details, Figures and so on. See DOI: 10.1039/b000000x/

1 M. Behrens, F. Studt, I. Kasatkin, S. Kühl, M. Hävecker, F. Abild-Pedersen, S. Zander, F. Girgsdies, P. Kurr, B.-L. Kniep, M. Tovar, R. W. Fischer, J. K. Nørskov and R. Schlögl, *Science*, 2012, **336**, 893-897.
2 Y.-H. Kim, J.-S. Heo, T.-H. Kim, S. Park, M.-H. Yoon, J. Kim, M. S. Oh, G.-R. Yi, Y.-Y. Noh and S. K. Park, *Nature*, 2012, **489**, 128-132.
3 M. Khajeh, S. Laurent and K. Dastafkan, *Chem. Rev*., 2013, **113**, 7728-7768.
4 W-.W. Zhan, Q. Kuang, J.-Z. Zhou, X.-J. Kong, Z.-X. Xie, and L.S. Zheng, *J. Am. Chem. Soc*., 2013, **135**, 1926-1933.
5 S. T. Kochuveedu, Y. H. Jang and D. H. Kim, *Chem. Soc. Rev.*, 2013, **42**, 8467-8493.
6 A. M. Schimpf, C. E. Gunthardt, J. D. Rinehart, J. M. Mayer and D. R. Gamelin, *J. Am. Chem. Soc*., **2013**, 135, 16569-16577.
7 S. Rawalekar and T. Mokari, *Adv. Energy Mater*., 2013, **3**, 12-27.
8 X. H. Cao, B. Zheng, X. H. Rui, W. H. Shi, Q. Y. Yan and H. Zhang, *Angew. Chem. Int. Ed*., 2014, **53**, 1404-1409.
9 F. E. Osterloh, *Chem. Soc. Rev.*, **2013**, 42, 2294-2320.
10 A. Kubacka, M. Fernandez-Garcia and G. Colon, *Chem. Rev.*, 2012, **112**, 1555-1614.
11 J. H. Yang, D. G. Wang, H. X. Han and C. Li, *Acc. Chem. Res.*, 2013, **46**, 1900-1909.
12 S. Cho, J.-W. Jang, K.-J. Kong, E. S. Kim, K.-H. Lee and J. S. Lee, *Adv. Funct. Mater*., 2013, **23**, 2348-2356.
13 T. Ohno, L. Bai, T. Hisatomi, K. Maeda and K. Domen, *J. Am. Chem. Soc*., 2012, **134**, 8254-8259.
14 S. R. Lingampalli, U. K. Gautam and C. N. R. Rao, *Energy Environ. Sci*., 2013, **6**, 3589-3594.
15 D. Koziej, A. Lauria and M. Niederberger, *Adv. Mater.*, 2014, **26**, 235-257.
16 Y. X. Liu, J. X. Shi, Q. Peng and Y. D. Li, *Chem. Eur. J*., 2013, **19**, 4319-4326.
17 D. E. Zhang, J. Y. Gong, J. J. Ma, G. Q. Han and Z. W. Tong, *Dalton Trans*., 2013, **42**, 16556-16561.

18 W. W. He, H.-K. Kim, W. G. Wamer, D. Melka, J. H. Callahan and J.-J. Yin, *J. Am. Chem. Soc*., 2014, **136**, 750-757.

19 Y. J. Wang, Q. S. Wang, X. Y. Zhan, F. M. Wang, M. Safdar and J. He, *Nanoscale*, 2013, **5**, 8326-8339.

20 S. T. Kochuveedu, Y. H. Jang, Y. J. Jang and D. H. Kim, *J. Mater. Chem. A*, 2013, **1**, 898-905.

21 A. Kargar, Y. Jing, S. J. Kim, C. T. Riley, X. Q. Pan and D. L.Wang, *ACS Nano*, 2013, **7**, 11112-11120.

22 S. Martha, K. H. Reddy and K. M. Parida, *J. Mater. Chem. A*, 2014, **2**, 3621-3631.

23 T. Surendar, S. Kumar and V. Shanker, *Phys. Chem. Chem. Phys.*, 2014, **16**, 728-735.

24 J.-D. Wang, J.-K. Liu, Q. Tong, Y. Lu and X.-H. Yang, *Ind. Eng. Chem. Res*., 2014, **53,** 2229-2237.

25 P. K. Sanoop, S. Anas, S. Ananthakumar, V. Gunasekar, R. Saravanan and V. Ponnusami, *Arab. J. Chem.*, 2014, *in press* (DOI: 10.1016/j.arabjc.2012.04.023).

26 S. Usai, S. Obregón, A. I. Becerro, and G. Colón, *J. Phys. Chem. C*, 2013, **117**, 24479-24484.

27 A. S. H. Hameed, C. Karthikeyan, S. Sasikumar, V. S. Kumar, S. Kumaresan and G. Ravi, *J. Mater. Chem. B*, 2013, **1**, 5950-5962.

28 D. P. Debecker and P. H. Mutin, *Chem. Soc. Rev*., 2012, **41**, 3624-3650.

29 Z. C. Hu, B. J. Deibert and J. Li, *Chem. Soc. Rev*., 2014, *in press* (DOI: 10.1039/c4cs00010b).

30 J. P. Huo, G. H. Deng, W. Wu, J. F. Xiong, M. L. Zhong and Z. Y. Wang, *Macromol. Rapid Commun.*, 2013, **34**, 1779-1784.

31 J. P. Huo, J. C. Luo, W. Wu, J. F. Xiong, G. Z. Mo and Z. Y. Wang, *Ind. Eng. Chem. Res*., 2013, **52**, 11850-11857.

32 K.-J. Kim, P. B. Kreider, C. Choi, C.-H. Chang and H.-G. Ahn, *RSC Adv*., 2013, **3**, 12702-12710.

33 L. Q. Fan, L. B. Liu, Y. W. Wang, H. Huo and Y. P. Xiong, *Int. J. Hydrogen Energy*, 2014, *in press* (DOI: 10.1016/j.ijhydene.2014.02.030).

34 F. Y. Wen and C. Li, *Acc. Chem. Res.*, 2013, **46**, 2355-2364.

35 P. Gao, Z. Y. Liu and D. D. Sun, *J. Mater. Chem. A*, 2013, **1**, 14262-14269.

36 C.Y. Su, C.T. Lu, W.T. Hsiao, W.H. Liu and F.S. Shieu, *Thin Solid Films*, 2013, **544**, 170-174.

37 Z. B. Zhan, Y. H. Wang, Z. Lin, J. Y. Zhang and F. Huang, *Chem. Commun*., 2011, **47**, 4517-4519.

38 P. Gomathisankar, K. Hachisuka, H. Katsumata, T. Suzuki, K. Funasakac and S. Kaneco, *RSC Adv*., 2013, **3**, 20429-20436.

39 P. Gomathisankar, K. Hachisuka, H. Katsumata, T. Suzuki, K. Funasaka and S. Kaneco, *ACS Sustainable Chem. Eng*., 2013, **1**, 982-988.

40 X. H. Lu, G. M. Wang, S. L. Xie, J. Y. Shi, W. Li, Y. X. Tong and Y. Li, *Chem. Commun*., 2012, **48**, 7717-7719.

41 Z. Hamdena, D. P. Ferreira, L. F. Vieira Ferreira and S. Bouattour, *Ceram. Int*., 2014, **40**, 3227-3235.

42 F. Z. Liu, Y. H. Leung, A. B. Djurišić, A. M. C. Ng and W. K. Chan, *J. Phys. Chem. C*, 2013, **117**, 12218-12228.

43 M. Kong, Y. Z. Li, X. Chen, T. T. Tian, P. F. Fang, F. Zheng and X. J. Zhao, *J. Am. Chem. Soc*., 2011, **133**, 16414-16417.